Original Contribution

Kurume Medical Journal, 62, 59-66, 2015

Interaction between Macrophages and Fibroblasts during Wound Healing of Burn Injuries in Rats

TAKESHI OKA, KEISUKE OHTA, TOMONOSHIN KANAZAWA AND KEI-ICHIRO NAKAMURA

Department of Anatomy, Kurume University School of Medicine, Kurume 830-0011, Fukuoka, Japan

Received 30 November 2015, accepted 24 December 2015
J-STAGE advance publication 25 May 2016

Edited by TAKEKUNI NAKAMA

Summary: Analysis of the structural changes and cell-to-cell interactions occurring during wound healing of burn injuries is essential to elucidate the morphological characteristics of the reconstitution of tissue architecture. However, conventional approaches do not provide sufficient information with respect to cell-to-cell interactions during wound healing. The aim of this study was to evaluate the interaction between bone marrow-derived cells and resident stromal cells throughout the wound healing of burn injuries, using immunohistochemistry and focused ion beam/scanning electron microscope tomography. We induced third-degree burn injuries on the backs of Wistar rats with a heated cylindrical aluminum block (2.0 cm in diameter). At 7 and 14 days after the burn injuries, the burned skin was immunostained with anti-Iba1 and anti-HSP47 antibodies for visualization of bone marrow-derived cells/macrophages and resident stromal cells/fibroblasts, respectively. Normal skin tissue was used as a control. Double-staining immunohistochemistry revealed frequent contacts between macrophages and fibroblasts and a higher contact ratio in the 3 normal skin compared with burned skin, particularly in the areas of granuloma. Three-dimensional ultrastructural analysis with focused ion beam/scanning electron microscope tomography revealed that macrophages and fibroblasts were located closer together in the normal skin than in the burned skin, confirming the analysis by light microscopic observations and ultrastructural analysis from single sections. These results highlight the importance of contact between macrophages and fibroblasts in the maintenance of skin tissue structure and during wound healing.

Key words burn injury, contact ratio, focused ion beam/scanning electron microscope tomography, immunohistochemistry, wound healing

INTRODUCTION

Following burn injury, damaged skin initiates healing processes to restore its integrity, which can be divided into three main phases: (1) inflammatory, (2) proliferative, and (3) remodeling [1,2]. Within each phase, a myriad of orchestrated reactions and interactions between cells and chemical factors occur [1-3]; however, there is considerable overlap between each phase, making them difficult to clearly delineate. Inflammatory mediator cells have been reported to play a role in wound healing [1-7]. In general, inflammation is observed in the wound area at 3-5 days after injury. During the later stages of inflammation, macrophages migrate into the wound and phagocytose the necrotic tissue and apoptotic neutrophils. At 14-21 days after injury, during the proliferative phase, macrophages migrate into the lesion, release cytokines, and stimulate fibroblast proliferation. In this phase, the extent of contact between macrophages and fibrob-

Corresponding author: Kei-ichiro Nakamura, Department of Anatomy, Kurume University School of Medicine 67 Asahi-machi, Kurume city, Fukuoka, Japan 830-0011. Tel: +81-942-31-7541 Fax: +81-942-31-7555 E-mail: ana2nkmr@med.kurume-u.ac.jp

Abbreviations: ECM, extracellular matrix; FIB, focused ion beam; HSP47, heat shock protein 47; Iba1, ionized calcium-binding adapter molecule 1; PBS, phosphate-buffered saline; PFA, paraformaldehyde; SEM, scanning electron microscopy; TEM, transmission electron microscopy; 3D, three-dimensional

lasts may mediate important signal transduction between these cells. Previous studies have described the modes of cell attachment and expression patterns of adhesion molecules based on immunological events after burns and mechanical injuries. Most of these studies examining cell-to-cell interactions and expression of intercellular adhesion molecules at the wound area have been performed using transmission and scanning electron microscopy (TEM and SEM, respectively) [8,28]. However, such classical two-dimensional observations of single sections at the ultrastructural level by TEM and tissue surface observations by SEM are not sufficient for a detailed evaluation of the cell-to-cell interactions of the entire structure.

Therefore, in the present study, we evaluated the histological changes that occur during wound healing of third-degree burn injuries in rats using immunohistochemistry and three-dimensional (3D) analysis with focused ion beam (FIB)/SEM tomography. The latter method could provide detailed ultrastructural information on the specimens at a higher resolution than possible with light microscopy and over a wider area than is feasible to visualize with ordinary TEM.

MATERIALS AND METHODS

Animal burn injury model

Nine male Wistar rats (10 weeks old, 310-360 g) were used to establish the burn model in this study. The rats were obtained from Kyushu Doubutsu Co. in accordance with the guidelines established by the Institutional Animal Committee of Kurume University School of Medicine. Animals were divided into 3 groups: normal control, 7 days after injury, and 14 days after injury. These time points were selected because they represent the transition from the inflammatory to proliferative phase of healing.

All experiments were performed when the animals were under deep anesthesia using diethyl ether and sodium pentobarbital (50 mg/kg). After the backs of the rats were shaved, an aluminum cylindrical block (2.0 cm in diameter) was heated in boiling water and placed onto the back of each animal for 20 s to cause the burn injury [10-13]. To avoid dehydration and infection, the wounds were covered with antibiotic ointment and artificial dermis (Terdermis, Thermo Scientific, Tokyo, Japan). The animals were allowed to move freely in their cages after surgery.

Immunohistochemistry/light microscopy

A total of six rats were used for immunohistochemical and light microscopy analysis. The targets, ionized calcium-binding adapter molecule 1 (Iba1) and heat shock protein 47 (HSP47), were chosen as markers of macrophages and fibroblasts, respectively. Iba1 was originally used as a marker for microglia but was recently recognized as a pan-macrophage marker [19-20], and has been widely used to identify macrophages within burned skin [21-22]. On the other hand, HSP47 is a 47-kDa heat shock protein that acts as a collagen-specific molecular chaperone [14-16], and was chosen for identification of fibroblasts rather than the commonly used fibroblast marker alpha-smooth muscle actin, because we aimed to identify all fibroblasts rather than only myofibroblasts [17-18]. In addition, alpha-smooth muscle actin antibody immunostaining may be less specific, with potential to also stain the vascular smooth muscle cells in the granuloma tissue. After 7 or 14 days, skin sections from the backs of the rats containing the wounds areas were obtained after fixation by transcardial perfusion with 2% paraformaldehyde (PFA) (pH 7.4) in phosphate-buffered saline (PBS) (pH 7.4) followed by incubation with heparinized (10 U/mL) saline. Resected specimens were immersed overnight in 30% sucrose in PBS and subsequently embedded and frozen in optimum cutting temperature compound (Sakura Tissue-Tek, Tokyo, Japan). Frozen specimens were cryosectioned into 10-μm-thick sections, and mounted on glass slides coated with poly-L-lysine. The sections were washed three times with PBS and blocked using a solution containing 1% gelatin and 0.1% Triton X-100 in PBS. The tissues were then incubated with rabbit anti-Iba1 antibody (1:5000 dilution; Wako, Osaka, Japan) and mouse anti-HSP47 antibody (1:1000 dilution; clone M16.10A1; Enzo Life Science, Farmingdale, NY, USA) overnight at 4°C. After three washes in PBS (pH 7.4), the sections were allowed to react with a secondary antibody mixture comprising goat anti-mouse IgG conjugated with Alexa488 Fluor (1:400 dilution, Molecular Probes, Eugene, OR, USA) and goat anti-rabbit IgG conjugated with Alexa568 Fluor (1:400 dilution; Molecular Probes) for 2 h at room temperature. Nuclei were counterstained with 4'-6-diamino-2-phenylindole. The processed sections were then observed under a confocal laser-scanning microscope (FV-1000; Olympus, Tokyo, Japan) at 600× magnification, and images were recorded. The macrophages and fibroblasts identified to be Iba1-immunoreactive (IR) and HSP47-IR at the wound areas were analyzed.

For semi-quantitative analysis of the contact ratio between macrophages and fibroblasts, 30 fields of view in the images were randomly selected from each der-

mis section (normal, and 7 and 14 days after injury). The numbers of Iba1-IR and HSP47-IR cells were counted, and the contact ratio between these cells was calculated as the number of contact points between the two signals divided by the total number of Iba1-IR and HSP47-IR cells, using Image J software (National Institutes of Health, Bethesda, MD, USA).

FIB/SEM tomography

Three rats were used for the ultrastructural analysis of normal skin and burn injury tissues with electron microscopic resolution. Tissues were transcardially fixed with 4% PFA in 2.5% glutaraldehyde, further fixed in the same fixative after resection, and then post-fixed using a combination of the ferrocyanide-reduced osmium method and the osmium-thiocarbohydrazide-osmium method to enhance membrane contrast, as follows [23]. After three washes in cacodylate buffer, the specimens were post-fixed for 2 h in a solution containing 2% osmium tetraoxide and 1.5% potassium ferrocyanide in cacodylate buffer at 4°C. The specimens were then washed three times with distilled water and immersed in 1% thiocarbohydrazide solution for 1 h.

After five washes with distilled water, the specimens were further immersed in 2% osmium tetraoxide in distilled water. After washing three times with distilled water, the specimens were en bloc-stained in a

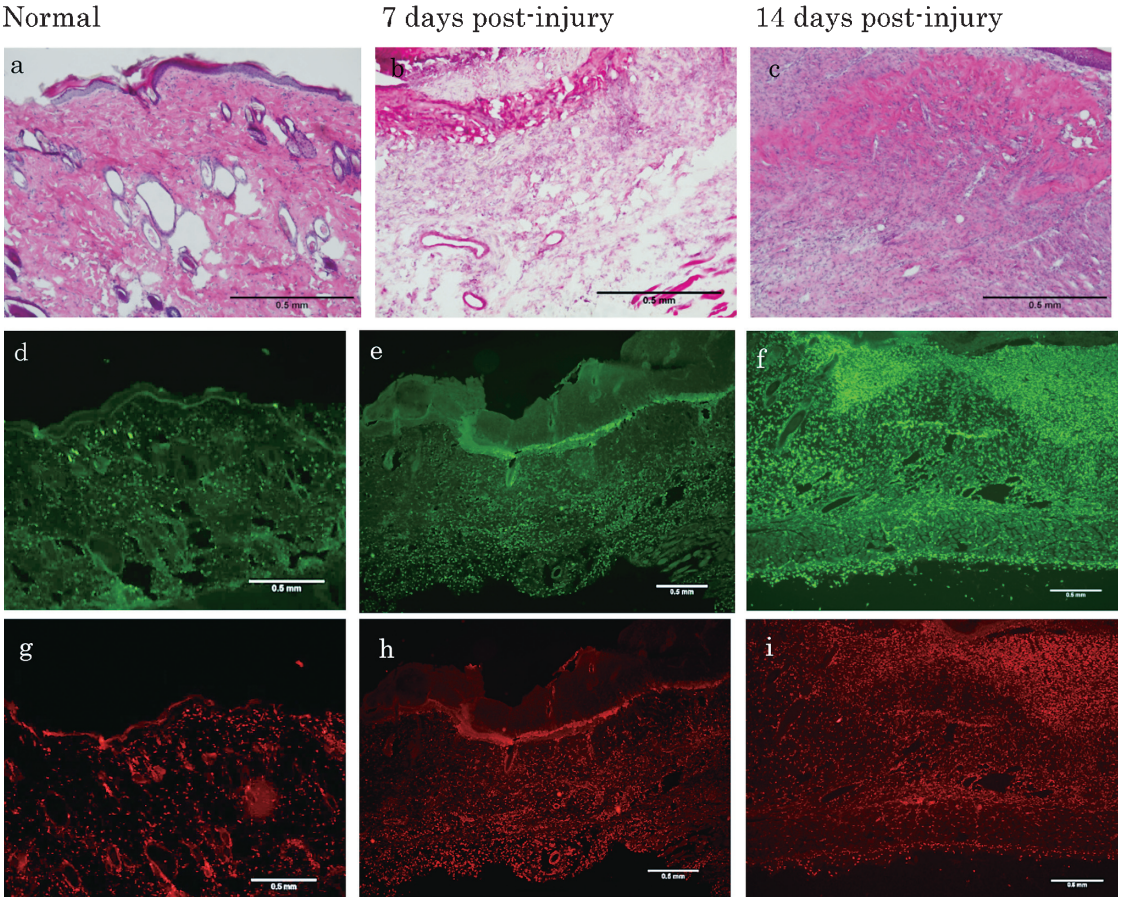

Fig. 1. (a-c) Light microscopic images of burned tissue sections stained with hematoxylin and eosin. Images from the left to right are from normal skin, burned skin at 7 days post-injury, and burned skin 14 days post-injury. At 7 days post-injury, infiltration of inflammatory cells was confirmed at the border between necrotic tissue and granulation tissue. At 14 days post-injury, the numbers of inflammatory cells was reduced more than observed in normal skin. Furthermore, the eosin-positive area had increased compared to that in normal skin. Scale bar = 0.5 mm. (e-i)

Immunostaining of burned tissue with monoclonal antibodies. Red: HSP47 (fibroblasts); green: IBA-1 (macrophages). At 7 days post-injury, both types of cells had infiltrated the border between the necrotic tissue and granulation tissue, especially around the blood vessels. At 14 days post-injury, granulation tissue occupied the upper region of the wound area, and the collagen fiber bundles appeared at the lower region of the wound area.

solution of 4% uranyl acetate dissolved in a 25% methanol solution overnight for contrast enhancement. After washing with distilled water, the specimens were dehydrated in an ethanol series (25%, 50%, 70%, 80%, 90%, and twice at 100% for 10 min each) followed by infiltration with an epoxy resin (EPON 812, TAAB, England, UK) and polymerization for 72 h at 60°C [23]. The resin blocks were trimmed down into a 2 × 5 mm area, and one surface was exposed using a diamond knife. The exposed surface, referred to as the block surface, was then coated with a thin layer of evaporated carbon to prevent charging and examined for backscattered electron imaging using field emission-SEM (Quanta 3D FEG FEI, the Netherlands). Serial images of the block face were acquired by repeated cycles of sample surface milling and imaging using Slice & View G2 operating software (FEI). For the reconstruction, the milling pitch of each image was set at 100 nm/cycle and the total size of the reconstruction volume was 100 × 100 × 60 μm. Specimen surface milling was performed with a gallium ion beam at 30 kV with a current of 100 pA. The image acquisition parameters using SEM were as follows: beam current = 46 pA, dwell time = 10 μs/pixel, image size = 2048 × 1768 pixels, (93.2 × 80.4 μm), pixel size = 45.5 nm/pixel. The resulting image stack was analyzed using Avizo 6.3 software (VSG Inc., Bordeaux, France).

Statistical analysis

Data for the number of IR cells and the contact ratio between Iba1-IR and HSP47-IR signals in the immnohistochemical analysis are presented as means ± standard error of the means and were analyzed by Kruskal-Wallis and Wilcoxon tests for multiple comparisons using JMP 10.0 for Windows (SAS Institute, Inc., Cary, NC, USA). Differences with p-values of less than 0.05 were considered statistically significant.

RESULTS

Immunohistochemical analysis of cell morphology

Infiltration of inflammatory cells into the border between granuloma tissue and necrotic tissues was confirmed through light microscopy of hematoxylin and eosin-stained samples collected 7 days after burn injury. Furthermore, the eosin-positive area increased at 14 days after burn injury (Figs. 1a–c).

In samples collected at 14 days after burn injury, compared to the normal skin, the number of inflammatory cells and Iba1-IR signals had decreased (Fig. 1f), and the necrotic areas were reduced, whereas the number of HSP47-IR signals had increased in the burned skin (Fig. 1i).

Double immunohistochemical staining for assessment of contact between Iba1-IR and HSP47-IR

Iba1-IR and HSP47-IR signals were frequently situated in close proximity in the normal skin samples (Figs. 2a). However, in the burned skin samples, the contact ratio for the two types of IR signals decreased at 7 days and was lowest at 14 days (Fig. 2b and 2c).

Semi-quantitative analysis of the contact ratio between Iba1-IR and HSP47-IR

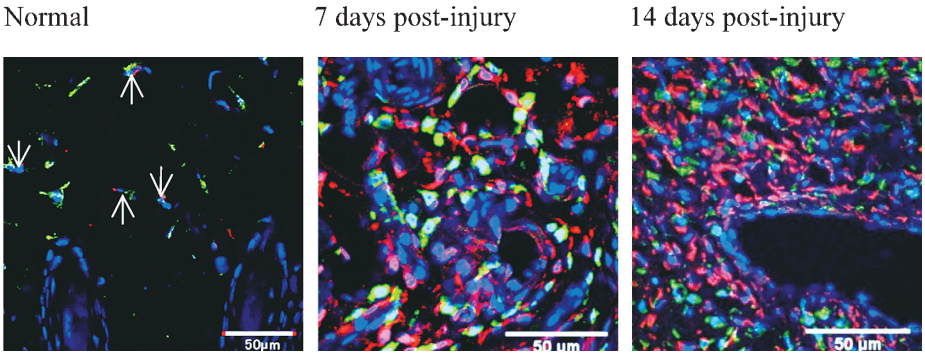

Fig. 2. Double immunochemical staining of normal skin and burned skin at 7 and 14 days post-injury. Red: HSP47 (fibroblasts); green: IBA-1 (macrophages); blue: DAPI (nucleus, arrows)

The contact ratio between IBA-1-positive cells and HSP47-positive cells was high in normal skin. In burned skin at 7 days post-injury, the macrophages–fibroblasts contact ratio was lower in the burned area than in the normal area. In burned skin at 14 days post-injury, the macrophages–fibroblasts contact ratio was higher than that at 7 days post-injury.

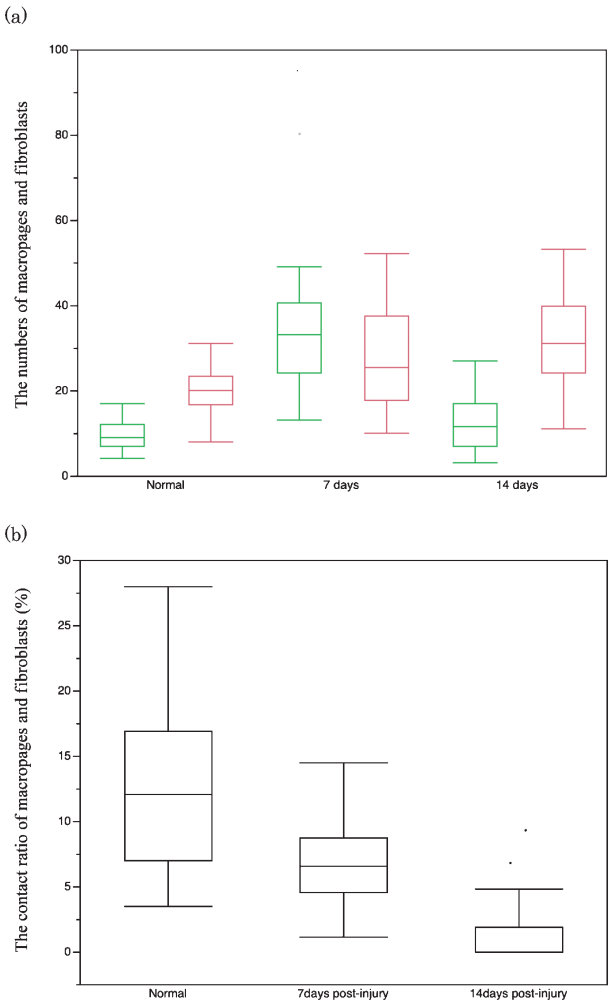

Fig. 3. Boxplot graphs showing (a) The numbers of macrophages (green) and fibroblasts (red) at 7 and 14 days following the burn injury. (b) The contact ratio of dermal macrophages and fibroblasts at each time point after a burn injury. The contact ratios of macrophages and fibroblasts decreased gradually ($P < 0.01$).

At 7 days after burn injury, the number of both Iba1-IR and HSP47-IR signals both increased in the burned injury skin compared to that in normal skin, but only the difference for Iba1-IR signals was statistically significant ($P < 0.01$). However, at 14 days after injury, the number of Iba1-IR signals in the burned skin showed a decrease compared to that observed in normal skin ($P = 0.068$), whereas

HSP47-IR signals were significantly enhanced in the burned skin compared to that in normal skin ($P < 0.01$; Fig. 3a).

The contact ratio for Iba1-IR and HSP47-IR signals was significantly greater in normal skin ($P < 0.01$), and showed a proportion decrease with length of time after injury, with ratios of 12.55%, 6.79%, and 1.24% for normal skin, at samples at 7 and 14 days after injury, respectively (Fig. 3b).

FIB/SEM tomographic analysis of cell morphology and cell-to-cell contact

Images obtained from FIB/SEM tomography showed reticular layers of the dermis in normal skin, and around newly formed vessels in the granuloma of burned skin. In the reconstructed images, cells with lysosome-rich cytoplasm were identified as macrophages, and cells with long cellular processes and endoplasmic reticulum-rich cytoplasm were identified as fibroblasts. Collagen fibers were closely packed in normal skin, but were sparse in burned skin. Two-dimensional images of single sections showed that the cells made contact in both normal skin and burned skin. The 3D images obtained via FIB/SEM tomography revealed large areas in which macrophages and fibroblasts were in contact. In normal skin, the contact area was broad and smooth, whereas that in burned skin was narrow and sharp. However, junctional structures such as desmosomes and gap junctions were not identified in any samples (Fig. 4).

DISCUSSION

In this study, we aimed to evaluate the interaction between Iba1-IR (as a macrophage marker) and HSP47-IR (as a fibroblast marker) throughout the two main phases of burn healing. The degree of contact between macrophages and fibroblasts was reduced in burned skin compared with that in normal skin, highlighting the importance of contact between these cells for the maintenance of skin tissue during wound healing.

During wound healing of burn injuries, granulation tissue appears at the wounded areas, which contain newly formed vessels, macrophages, fibroblasts, and extracellular matrix (ECM) [1,6,7]. Macrophages play important roles in the healing process because of their ability to secrete various types of cytokines and chemokines. In addition, macrophages can migrate into the wound within 48-96 h after injury to help neutrophils complete debridement in order to terminate the inflammatory response [2]. Both the ECM, including type Ⅲ collagen, and the number of fibroblasts have been reported to increase in burned skin at 7 days after injury [1-6]. Furthermore, at 14 days after injury, myofibroblasts, which express alpha-smooth muscle actin and have the capacity for active motility, have also been observed at the edge of the granulation tissue [7].

In the present study, double immunohistochemical staining and concomitant statistical analysis confirmed

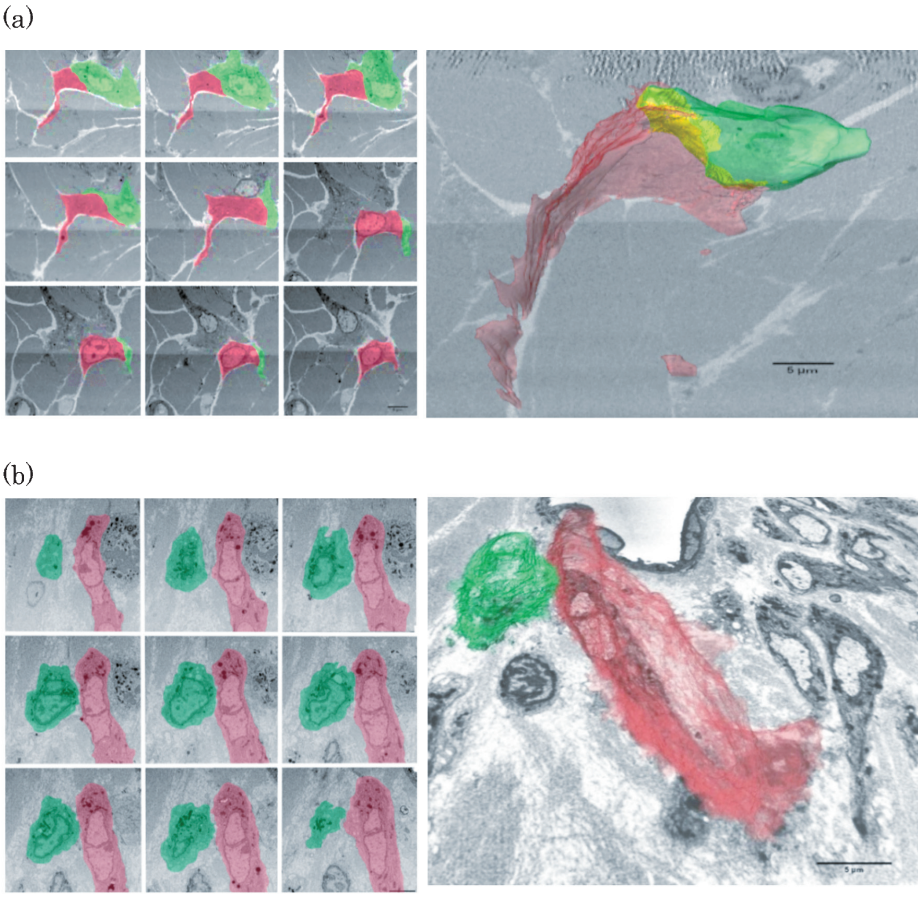

Fig. 4. A series of scanning electron microscope (SEM) images are shown on the left, and the images reconstructed from three-dimensional focused ion beam/scanning electron microscope tomography are shown on the right. The images on top are from normal skin, and the images on the bottom are from burned skin. The space between the SEM images is 1.5 μm. Green indicates macrophages, red indicates fibroblasts, and yellow indicates the contact area. Scale Bar, 5 μm.
Normal 7 days post-injury 14 days post-injury

the results obtained from a previous study, showing that the numbers of immune cells and fibroblasts in the normal dermis (excluding the blood vessels and nerve bundles) are similar, revising the previous notion that the main constituent of the dermis is fibroblasts [2-6].

We also clearly revealed the dynamics of the contact ratios between normal and burned skin; the numbers of Iba1-immunopositive macrophages increased significantly at 7 days after burn injury and then decreased at 14 days, whereas the number of HSP47-immunopositive fibroblasts increased gradually until day 14. We assumed that the histopathological features observed at 7 days after burn injury represent the transitional phase from the inflammatory phase to the proliferative phase, while those at 14 days after injury represented the peak of the proliferative phase. This, together with data from previous reports [1-6], encouraged us to choose these two time points of 7 and 14 days after burn injury for evaluating the cytological characteristics of these two phases during recovery from burn injuries.

Thus, to examine the importance of cell-to-cell interaction or direct attachment between macrophages and fibroblasts, we focused on the contact ratio between these cells as a measure of cell-to-cell interaction. Previous studies have mostly evaluated the role of cell-to-cell interactions in burn injuries based on TEM and SEM as well as analysis of intercellular adhesion molecules in wounded areas [8-10]. For example, Steinhauser et al. [9] observed significant upregulation in the chemokine macrophage inflammatory protein 1-alpha in a co-culture system consisting of macrophages layered over confluent fibroblasts. On the other hand, White et al. [10] reported that the expression levels of

transforming growth factor-beta-1, vascular epidermal growth factor, and type I collagen mRNA significantly increased in fibroblasts after incubation with macrophage cultures.

These findings indicate that the transmission of specific information from macrophages to fibroblasts is essential in normal skin and that this activity is reduced at the proliferative phase. Moreover, such information transmission appears to be important for maintaining integrity of the connective tissue [8-10]. The present study provides the first quantitatively comparison of the contact ratio of macrophages and fibroblasts between normal skin and burned skin. This factor may provide important insights into the mechanisms involved in the restoration of connective tissue.

The particular mode of cell-to-cell contact is also an important factor to consider with respect to healing in addition to the degree of contact. However, technical limitations have thus far prevented the study of these features in detail. Furthermore, two-dimensional images of single sections are generally inadequate for determining the entire structure of the focal contact between these cells, even regarding simple matters such as whether or not the contact areas are large or narrow. In the present study, we were able to observe the 3D structures of cell-to-cell contacts using FIB/SEM tomography, and revealed the 3D mode of cell-to-cell contact between macrophages and fibroblasts at the ultrastructural level. The consequent 3D images enabled us to analyze the spatial morphological relationships of cell-to-cell interactions, because we could clearly visualize a wider area than possible using TEM [26]. Therefore, we were able to reconstruct the 3D morphology from serial images, which permitted reconstruction at the level of the desired angle to obtain an optimal two-dimensional view with which to reveal the fine structure of the specimens.

The normal structure of the dermis from human specimens was previously described with the FIB/SEM technique. Recently, Cretoiu et al. [27] used FIB/SEM tomography to describe the structure of human skin telocytes, which provide a winding path from the interstitial cells of Cajal. However, only normal skin tissue was analyzed, and burned skin was not assessed or compared. In the present study, the 3D images showed that the mode of contact between macrophages and fibroblasts in burned skin was narrow and showed a pattern of point-to-point contact in some cases; the SEM images demonstrated close contacts between the two cell types. Moreover, FIB/SEM tomography showed that the contact area was much larger in the normal skin than in burned skin, suggesting that cellular contact is advantageous to signal transduction. Shekhter et al. [8] reported an interaction between macrophages and fibroblasts in granuloma tissue. Thus, the results of our study differ from this previous report; this apparent conflict may be associated with technical differences. In particular, their study involved precise observations of several single sections, whereas, we obtained 3D images of whole cells using FIB/SEM tomography.

Evidence that has accumulated to date points to the general importance of close cell-to-cell apposition or contact and gap junctional connections for maintaining tissue structure and function [28,29]. Unfortunately, we were not able to confirm the detailed structures of the attachments or gap junctions in this study; thus, future studies are needed to determine the microstructures of collagen attachments.

In conclusion, we demonstrated that the contact ratio and mode of contact between macrophages and fibroblasts differed between normal and burned skin, indicating that the mode of contact might serve a specific function in skin maintenance or wound healing. This factor presumably reflects the mechanisms underlying the transmission of specific information via the catabolism and biosynthesis of connective tissue, particularly collagen fibers, carried out in normal skin.

REFERENCES

1. Falabella AF and Falanga V. Wound healing In: Freinkel RK, Woodley D T. Eds. The biology of the skin, New York. The Parthenon Publish Group Inc. 2001; 281-297.
2. Broughton G, Janis JE, and Attinger CE. The basic science of wound healing. Plast Reconstr Surg. 2006; 117:12S-34S.
3. Eming SA, Kreig T, and Davidson JM. Inflammation in wound repair, molecular and cellular mechanism. J Invest Dermatol. 2007; 127:514-525.
4. Driskell RR, Lichtenberger BM, Hoste E, Kretzschmar K, et al. Distinct fibroblast lineages determine dermal architecture in skin development and repair. Nature 2013; 504: 277-281.
5. Natsuaki Y, Egawa G, Nakamizo S, Ono S, Hanakawa S et al. Perivascular leukocyte clusters are essential for efficient activation of effector T cell in the skin. Nat Immunol. 2014; 15:1064-1071.
6. Hinz B. Formation and function of the myofibroblast during tissue repair. J Invest Dermatol. 2007; 127:526-537.
7. Kibe Y, Takenaka H, and Kishimoto S. Spatial and temporal expression of basic fibroblast growth factor protein during wound healing of rat skin. Br J Dermatol. 2003; 143:720-727.
8. Shekhter AB, Berchenko GN, and Nikolaev AV. Macrophage-fibroblast interaction and its possible role in the regulation of collagen metabolism during wound healing. Bull Exsp Biol Med. 1977; 83:627-630.
9. Steinhauser ML, Kunkel SL, Cory M, Hogaboam CM,

Evanoff H et al. Macrophage/fibroblast coculture induces macrophage inflammatory protein-1alpha production mediated by intercellular adhesion molecule-1 and oxygen radicals. Leukoc Biol. 1998; 64:636-641.
10. White JC, Jiang ZL, Diamond MP, and Saed GM. Macrophages induce the adhesion phenotype in normal peritoneal fibroblasts. Fertil and Steril 2011; 96:758-763.
11. Yamaguchi R, Takami Y, Yamaguchi Y, and Shimazaki S. Bone marrow-derived myofibroblasts recruitd to the upper dermis appear beneath regenerating epidermis after deep dermal burn injury. Wound Repair Regen. 2007; 15:87-93.
12. Wang J, Li D, Xia F, Tu YY, and Huang XY. Histological and biomechanical evaluation of the preserved degenerative dermis in rat autologous skin transplant models after a deep second degree burn. Scand J Lab Anim Sci. 2009; 36: 139-145.
13. Romana-Souza B, Nascimento AP, and Monte-Alto-Costa A. Low-dose propranolol improves cutaneous wound healing of burn-injured rats. Plastic Reconstr Surg. 2006; 112: 1690-1699.
14. Kuroda K and Tajima S. HSP47 is a useful marker for skin fibroblasts in formalin-fixed, paraffin-embedded tissue specimens. J Cutan Pathol. 2004; 31:241-246.
15. Kuroda K and Tajima S. Proliferation of HSP47-positive skin fibroblasts in dermatofibroma. J Cutan Pathol. 2008; 35:21-26.
16. Wang Z, Inokuchi T, Nemoto TK, Uehara M, and Baba TT. Antisense oligonucleotide against collagen-specific molecular chaperone 47-kDa heat shock protein suppresses scar formation in rat wounds. Plast Reconst Surg. 2003; 111: 1980-1987.
17. Akasaka Y, Ono I, Tominaga A, Ishikawa W, Ito K et al. Basic fibroblast growth factor in an artificial dermis promotes apoptosis and inhibits expression of alpha-smooth muscle actin leading to reduction of wound contraction. Wound Repair and Regen. 2007; 15:378-389.
18. Ishiguro S, Akasaka Y, Kiguchi H, Suzuki T, Imaizumi R et al. Basic fibroblast growth factor induces down-regulation of alpha-smooth muscle actin and reduction of myofibroblast areas in open skin wounds. Wound Repair Regen. 2009; 17: 617-625.
19. Ishida Y, Gao JL, and Murphy PM. Chemokine receptor CX3CR1 mediates skin wound healing by promoting macrophage and fibroblast accumulation and function. J Immunol. 2008; 180:569-579.
20. Erez N, Truitt M, Olson P, Arron ST, and Hanahan D. Cancer-associated fibroblasts are activated in incipient neoplasia to orchestrate tumor-promoting inflammation in an NF-κB-dependent manner. Cancer Cell. 2010; 17:135-147.
21. Ito D, Tanaka K, Suzuki S, Dembo T, and Fukuuchi Y. Enhanced expression of Iba1, ionized calcium-binding adapter molecule 1, after transient focal cerebral ischemia in rat brain. Stroke 2001; 32:1208-1215.
22. Ohsawa K, Imai Y, Kanazawa H, Sasaki Y, and Kohsaka S. Involvement of Iba1 in membrane ruffing and phagocytosis of macrophages/microglia. J Cell Sci. 2000; 113:3073-3084.
23. Villinger C, Wanner G, and Walther P. FIB/SEM tomography with TEM-like resolution for 3D imaging of high-pressure frozen cells. Histochem Cell Biol. 2012; 138:549-556.
24. Ohta K, Sadayama S, Togo A, Higashi R, Tanoue R et al. Beam deceleration for block-face scanning electron microscopy of embedded biological tissue. Micron. 2012; 43:612-620.
25. Knott G, Marchman H, Wall D, and Lich B. Serial section scanning electron microscopy of adult brain tissue using focused ion beam milling. J Neurosci. 2008; 28:2959-2964.
26. Ichimura K, Miyazaki N, Sadayama S, Murata K, Koike M et al. Three-dimensional architecture of podocytes revealed by block-face scanning electron microscopy. Sci Rep. 2015; 5:8993.
27. Cretoiu D, Gherghiceanu M, Hummel E, Zimmermann H, Simionescu O et al. FIB-SEM tomography of human skin telocytes and their extracellular vesicles. J Cell Mol Med. 2015; 19:714-722.
28. Takayama T, Kondo T, Kobayashi M, Ohta K, Ishibashi Y et al. Characteristic morphology and distribution of bone marrow derived cells in the cornea. Anat Rec. (Hoboken) 2009; 292:756-763.
29. Ueda A, Nishida T, Otori T, and Fujita H. Electron-microscopic studies on the presence of gap junctions between corneal fibroblasts in rabbits. Cell Tissue Res. 1987; 249:473-475.